

See discussions, stats, and author profiles for this publication at: <https://www.researchgate.net/publication/50913797>

A Wavefunction-Based Criterion for the Detection of Intermolecular Interactions in Molecular Dynamics Simulations

ARTICLE *in* THE JOURNAL OF PHYSICAL CHEMISTRY A · APRIL 2003

Impact Factor: 2.69 · DOI: 10.1021/jp027247y · Source: OAI

CITATIONS

17

READS

48

2 AUTHORS:



Markus Reiher

ETH Zurich

289 PUBLICATIONS 8,497 CITATIONS

SEE PROFILE



Barbara Kirchner

University of Bonn

201 PUBLICATIONS 4,504 CITATIONS

SEE PROFILE

A Wavefunction-Based Criterion for the Detection of Intermolecular Interactions in Molecular Dynamics Simulations

Markus Reiher^{*,†} and Barbara Kirchner^{*,‡}

*Theoretische Chemie, Universität Erlangen-Nürnberg, Egerlandstrasse 3, D-91058 Erlangen, Germany, and
Physikalisch-Chemisches Institut, Universität Zürich, Winterthurerstrasse 190, CH-8057 Zürich, Switzerland*

Received: October 18, 2002; In Final Form: February 28, 2003

The availability of quantum mechanical wave functions in molecular dynamics simulations — for example in those of the Car–Parrinello type — offers the ability to analyze intermolecular interactions of a system in terms of quantum chemical descriptors. We demonstrate how standard population analyses can be utilized for a semiquantitative analysis of intermolecular interactions. The approach is therefore of particular value for the study of those systems for which geometric criteria and predefined interaction potentials have not yet been obtained. This is demonstrated for a DMSO–water mixture, for which the population-analysis criterion provides a simple measure for different interaction types, e.g., between water–oxygen and methyl–hydrogen atoms. In the case of a polypeptide, it is shown that the wave-function-based criterion provides insight into hydrogen bonding of the C=O groups with a hydrogen atom attached to a carbon atom from the peptide's backbone.

1. Introduction

Hydrogen bonds in hydrophilic and hydrophobic situations or in agostic interactions represent a key structure motif in chemistry.^{1–4} The understanding of these intra- and intermolecular interactions of medium strength is decisive for almost all chemical processes which take place, for instance, in solution, in a protein environment, or at a catalytic transition metal center. Molecular dynamics (MD) simulations of, for instance, liquid structures, molecular recognition in supermolecular and biochemistry, and drug design rely extensively on the interpretation of intermolecular interactions in terms of interaction energies.^{5–7} The standard approach for estimating interaction energies in large complex aggregates is based on geometric criteria, which solely defines the interaction of two fragments of an aggregate on the basis of distances (and occasionally of angles).⁵ It is most desirable to have a single descriptor for the interaction energy; however, this cannot easily be identified. Chandler noted, for example, that attempts on the quantification of predictions of protein structures with hydrophobic and hydrophilic amino acids “by identifying a single parameter or function that characterizes the strength of hydrophobic interactions have been unsuccessful”.⁸ Apart from practical problems with mapping of an interaction energy onto a single descriptor, we also face fundamental quantum mechanical difficulties: if an aggregate of two subsystems which interact with one another via more than one site, is decomposed into these two subsystems, the interaction energy for a single attractive site in the aggregate cannot be extracted from the total decomposition energy.

A wave-function-based criterion, as opposed to a geometric criterion, is desirable because it is sensitive to different environments in which the hydrogen bond is formed: (1) different acceptor atoms; (2) different donor atoms; (3) bifur-

cated hydrogen bonds; (4) weakening and/or strengthening of the hydrogen bond due to indirect influences which may be inter- or intramolecular; (5) solvent effects; and (6) many-body effects. All this cannot be detected by standard geometric criteria.

The dawn of first principles MD like Car–Parrinello MD (CPMD)⁹ allows for new descriptors for the interaction strength as the electronic structure — in addition to the so-called ionic positions of all atoms involved — is available at each time step. Of course, the above-mentioned fundamental problem that the interaction energy of a large cluster of molecules is not an observable quantity cannot be circumvented by the knowledge of the wave function. However, the wave function naturally tracks all electronic changes in an aggregate, and its analysis should yield very useful insight into the intermolecular interactions within the aggregate. Note that a wave-function-based descriptor would also be helpful in classical MD because snapshots of the ensemble can be calculated easily with advanced static quantum chemical methods.

For static quantum chemical calculations on optimized structures it has been found that the intramolecular hydrogen bond energy E_{HA} between pairs of hydrogen atoms H and acceptor atoms A can be estimated from a 2-center shared-electron number σ_{HA} (SEN),¹⁰ which is a single-valued descriptor for the electronic density between H and A:

$$E_{\text{HA}}^{\text{SEN}} = -\lambda \sigma_{\text{HA}} \quad (1)$$

This relationship represents the chemical picture of an increased bond strength upon an increased electronic density between the interacting atoms as has been demonstrated for covalent chemical bonds by Ehrhardt and Ahlrichs.¹¹ SEN is easily obtained from the wave function by population analysis.^{12–14} Here, we test the applicability of this concept for MD simulations and suggest considering σ_{HA} as the sought-for single descriptor for the interaction energy in (quantum chemically) nondecomposable systems and chemically different environ-

* Correspondence may be addressed to either author via e-mail: Markus.Reiher@chemie.uni-erlangen.de or kirchner@pci.unizh.ch.

[†] Universität Erlangen-Nürnberg.

[‡] Universität Zürich.

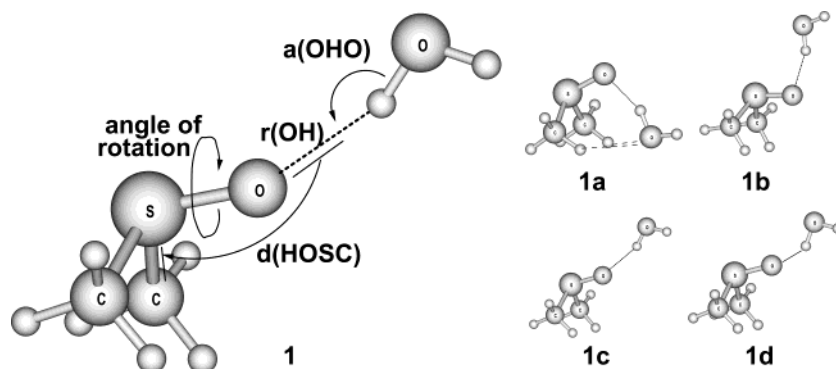


Figure 1. Typical clusters out of a DMSO–water mixture.

ments. In a first step, we demonstrate that SEN can be used as a probe on inter- and intramolecular interactions, which is especially valuable in those cases which would hardly be visible in an analysis purely based on geometric criteria. Then we analyze to which extent the linear relationship in eq 1 can be used for the quantitative calculation of interaction energies.

2. Quantum Chemical Methodology

For all calculations in this work we used the density functional programs provided by the TURBOMOLE 5.1 suite.¹⁵ We employed the hybrid DFT functional B3LYP^{16,17} for the all-electron Kohn–Sham calculations as implemented in TURBOMOLE. Ahlrichs’ TZVP basis set was used throughout, featuring a valence triple- ζ basis set with polarization functions on all atoms.¹⁸ All interaction energies calculated within the supermolecular approach, $E_{\text{HA}}^{\text{sup, cp}}$, have been counter-poise corrected^{19,20} for the basis set superposition error. For the analysis of the electronic wave function we made use of the concept of shared-electron numbers (SEN)¹⁴ as implemented in TURBOMOLE.

This Davidson–Roby–Ahlrichs population analysis is also implemented in the CPMD code²¹ of the Parrinello group.²² It is important to note that SEN analyses within such a CPMD-plane-wave framework do not suffer from the basis set superposition error because the basis set is *not* atom-centered.

Interaction energies, $E_{\text{HA}}^{\text{SEN}}$, are evaluated on the basis of two-center shared electron numbers between a hydrogen atom and the corresponding acceptor atom; see ref 10 for details on this approach. We should emphasize that the population analysis can be carried out easily and is thus very feasible in terms of computer time demands. Furthermore, even the quantum chemical calculation of single-point snapshots from a classical MD simulation are becoming more and more feasible because of recent advances in algorithmic techniques of the quantum chemical methods, such as density fitting and linear scaling approaches (see, for example refs 23–31).

3. Case I: Simulation of Complex Liquids

As an exemplary system we choose a mixture of dimethyl sulfoxide (DMSO) and water, which we have recently studied in terms of small clusters with standard quantum chemical methods³² and by CPMD simulations.³³ Figure 1 shows four configurations of one DMSO and one water molecule.

While configuration **1a** is the global minimum of this two-molecule system, **1b** represents a local minimum. The other two configurations, **1c** and **1d**, are nonminimum structures in the attractive and repulsive, respectively, regions of the potential energy curve for the hydrogen bond. Table 1 lists the calculated interaction energies obtained within the supermolecular ap-

TABLE 1: Benefits and Limits of the SEN Approach to Intermolecular Interaction Energies for the Clusters in Figure 1^a

	$r(\text{HA})$	$a(\text{OHO})$	$d(\text{HOSC})$	$E_{\text{H}_2\text{O}-\text{DMSO}}^{\text{sup, cp}}$	σ_{HA}	$E_{\text{H}(\text{H}_2\text{O})-\text{O}(\text{DMSO})}^{\text{SEN}}$
1a	182.4	156.3	−52.0	−40.0	0.0655	−33.7
1b	182.4	156.3	130.1	−27.9	0.0585	−30.1
1c	207.1	157.3	130.2	−21.5	0.0223	−11.5
1d	156.6	139.6	130.5	10.0	0.1013	−52.1

^a Distances are given in pm, angles are in degrees, and energies are in kJ/mol.

proach, $E_{\text{H}_2\text{O}-\text{DMSO}}^{\text{sup, cp}}$, and as obtained with the SEN method, $E_{\text{H}(\text{H}_2\text{O})-\text{O}(\text{DMSO})}^{\text{SEN}}$, according to eq 1.

Although the local minimum **1b** is very well described by $E_{\text{H}(\text{H}_2\text{O})-\text{O}(\text{DMSO})}^{\text{SEN}}$ when compared to the supermolecular reference energy, this seems not to be the case for the global minimum **1a**. However, this discrepancy originates from the fact that two additional attractive contacts to the methyl groups of DMSO have to be taken into account in $E_{\text{HA}}^{\text{SEN, tot}}$:

$$E_{\text{HA}}^{\text{SEN, tot}} = -\lambda \sum_{i=1}^n \sigma_{\text{HA}, i} \quad (2)$$

with $n = 3$ in this case. The $\sigma_{\text{HA}, i}$ contributions from the two $\text{O}(\text{H}_2\text{O}) \cdots \text{H}(\text{CH}_3)$ contacts amount to 2.6 kJ/mol each (according to their calculated SEN values of $\sigma_{\text{HA}, i} = 0.0050$). With these additional attractive contributions we obtain $E_{\text{HA}}^{\text{SEN, tot}} = -38.9$ kJ/mol, which is in good agreement with the −40.0 kJ/mol of the supermolecular approach.

Although the SEN method gives the interaction energy for the particular interaction under study, the supermolecular approach can — for the fundamental quantum mechanical reasons mentioned above — yield only the total interaction energy for all interactions involved in the system. Therefore, structure **1a** is very well described by the SEN approach if all relevant $\sigma_{\text{HA}, i}$ values are considered. Although SEN attributes an interaction energy to a pair of atoms, many-body effects of surrounding atoms on this pair of atoms are implicitly taken into account, as the population analysis required for the calculation of the $\sigma_{\text{HA}, i}$ starts from the *total* electronic wave function. These benefits are not given by a geometric criterion. A geometric criterion, even as applied in the more sophisticated cases, is not able to distinguish between configuration **1a** and **1b** because it monitors the hydrogen bond using distance and angle only. Even if a geometric criterion additionally would include the dihedral angle, it is not sensitive to the environment as already mentioned in the Introduction. Here, the environment is represented by the methyl groups.

For structure **1c** we find a larger deviation to the supermolecular interaction energy, because eq 1 is not well fulfilled

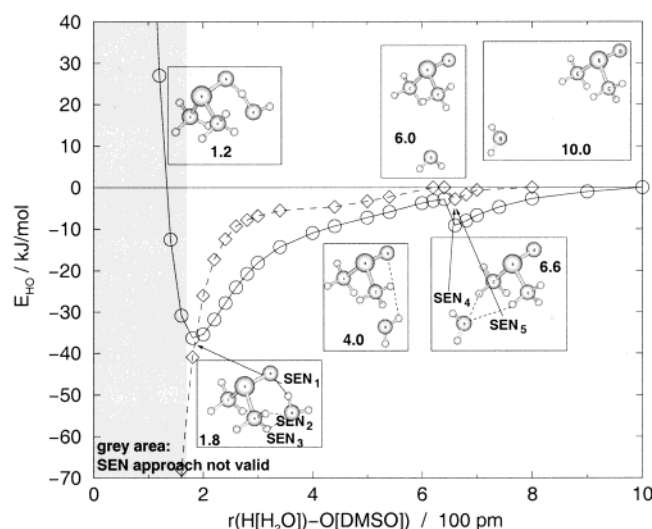


Figure 2. Domain of validity of the empirical relation between shared-electron number and counter-poise corrected supermolecular interaction energy (circles) in the DMSO–water cluster **1a**. The SEN has been linearly scaled (diamonds) with the parameter λ from ref 10 according to eq 1 in order to yield an energy scale for comparison. Note that the SEN interaction curve represents five different SENs which are important on different lengths scales: while SEN_1 – SEN_3 governs the short-range region of $r(\text{H}[\text{H}_2\text{O}]\cdots\text{O}[\text{DMSO}])$, SEN_4 and SEN_5 are important for the local minimum at larger distances. Both types of SENs do not interfere in these two domains and the given SEN interaction curve is thus a superposition of two independent SEN interaction curves (compare Figure 3).

for nonminimum structures. However, even in these cases the simple SEN approach defined by eq 1 can serve as a useful probe for the detection of interactions.

The case of **1d** demonstrates the limits of the SEN approach: the interaction energy is already positive, while the SEN value is still increased in a strongly repulsive region. The values of σ_{HA} will only drop down to zero if the two atoms H and A get very close. For this reason, the SEN criterion can be utilized only in nonrepulsive areas of the potential energy curve. Fortunately, the repulsive areas can be easily identified within the SEN approach, as the largest value allowed for σ_{HA} should be close to the value at the equilibrium distance. This maximum value for σ_{HA} can be obtained approximately for all possible interaction types involved in the system under study by calculating the small number of pair interaction potentials with static quantum chemical methods a priori to the MD simulation. Thus, there is no need to rely on geometric parameters within the SEN approach for the identification of the repulsive regions of the potential energy surface.

To illustrate the benefits and limits of SEN, Figure 2 shows the potential energy curve for cluster **1a**, which was obtained by increasing the DMSO–oxygen–water–hydrogen distance under full relaxation of the rest of the cluster and by the SEN approach (the corresponding SEN values are depicted in Figure 3).

Below a distance of 180 pm between DMSO–oxygen and water–hydrogen, the repulsive region is entered, where the true interaction energy is rapidly increasing while the SEN interaction energy is still dropping down. This region defines the SEN value at the equilibrium structure which must be taken as the maximally allowed value. The reconstruction of the attractive region of the potential energy curve from shared-electron numbers deviates from the true interaction potential. This has two reasons: (i) the reconstruction utilizes only those *five* SEN values for the five possible contacts between the water and the

DMSO molecules; it is thus a superposition of five SEN interaction curves mapped onto the same one-dimensional interaction coordinate; and (ii) the distance dependence of each of these five shared-electron numbers was not taken into account in the original setup for the SEN method in ref 10, for which only equilibrium structures were used. The accuracy of the reconstructed SEN potential curves could thus be improved by either performing a new adjustment, which also includes nonequilibrium structures, or including an explicitly distance-dependent term in the adjustment procedure. In the latter case, the angular dependence and the many-body effects are expected to be included through the SEN value in a complex system in such a way that the parameters of the fitting expression can be adjusted to *pair*-interaction data. In doing so, even statistical analyses could be made feasible.

A decisive aspect of Figure 2 is that the SEN approach is able to predict the two attractive $\text{O}(\text{H}_2\text{O})\cdots\text{H}(\text{CH}_3)$ contacts at 660 pm. At this DMSO–oxygen–water–hydrogen distance, the water molecule is caught by the two methyl groups from behind, which is again an example of an environmental effect. Although SEN has this capability also in a many-molecule system, neither the supermolecular approach nor geometric criteria are able to capture such a feature. The supermolecular approach cannot provide an interaction energy for each contact and would fail for a large many-molecule system for practical reasons (it would be unfeasible to calculate all molecules in a system in every time step to evaluate their total interaction energy). The geometric criterion fails because such an unexpected interaction is not included in the set of rules. Though the agreement between $E_{\text{HA}}^{\text{SEN,tot}}$ and $E_{\text{H}_2\text{O}-\text{DMSO}}^{\text{sup,cp}}$ in Figure 2 is not exact, weak and strong contacts of the same interaction type can still be identified on a semiquantitative basis.

Figure 4 shows a snapshot from a CPMD simulation of a DMSO–water mixture whose structure was taken from ref 33. This structure was then subjected to a population analysis using TURBOMOLE, and the resulting SEN values and corresponding attraction energies are given in Figure 4 for the inner core of the mixture.

This sample snapshot demonstrates that the SEN approach is capable of detecting even very weak interactions in this systems: the interaction energies range from -0.6 kJ/mol to -21.7 kJ/mol. Although a simulation under standard conditions usually contains structures of attractive nature there are also a few structures from the repulsive region. The three hydrogen bridges between water molecules, which are underlined in Figure 4, are already in the repulsive area of the interaction potential curve though their interaction energy may still be negative. They are easily identified by their SEN values of 0.0640, 0.0853, and 0.0605, which are much larger than the SEN value of $21.6/\lambda = 0.0420$ for the relaxed water dimer (21.6 kJ/mol being the B3LYP/TZVP interaction energy of the water dimer, and $\lambda = 514$ for B3LYP/TZVP). For these three hydrogen bonds, the SEN approach has thus not yet yielded a correct value for the interaction energy. Additional corrections to the simple expression in eq 1 are needed to correct for the behavior at distances which are slightly shorter than the equilibrium distance (the oxygen–hydrogen distances in these three cases are 181.6, 178.5, and 186.3 pm, respectively, whereas the B3LYP/TZVP equilibrium distance is 196.9 pm).

4. Case II: Polypeptides and Proteins

As a second example, we should like to demonstrate the usefulness of the SEN approach to biochemical systems. Hydrogen bonding in polypeptides and proteins is usually

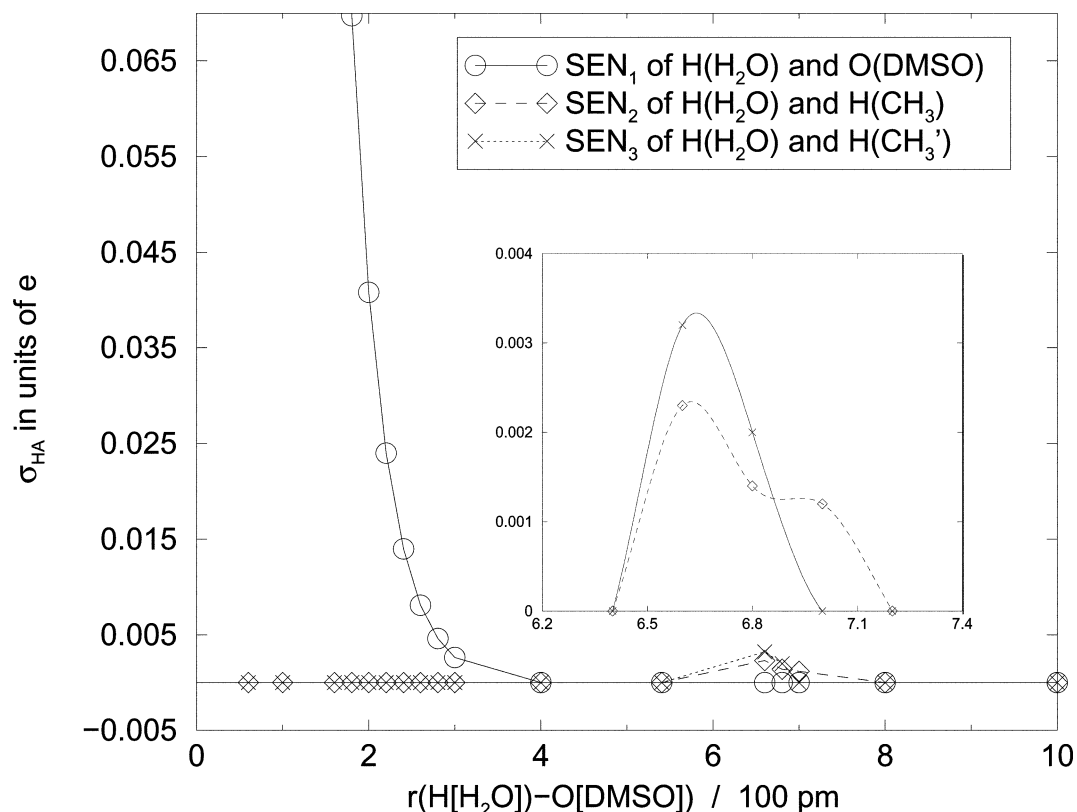


Figure 3. Values for the three shared-electron numbers SEN_1 , SEN_4 , and SEN_5 , which were used for the calculation of the $E_{HA}^{SEN,tot}$ potential energy curve in Figure 2.

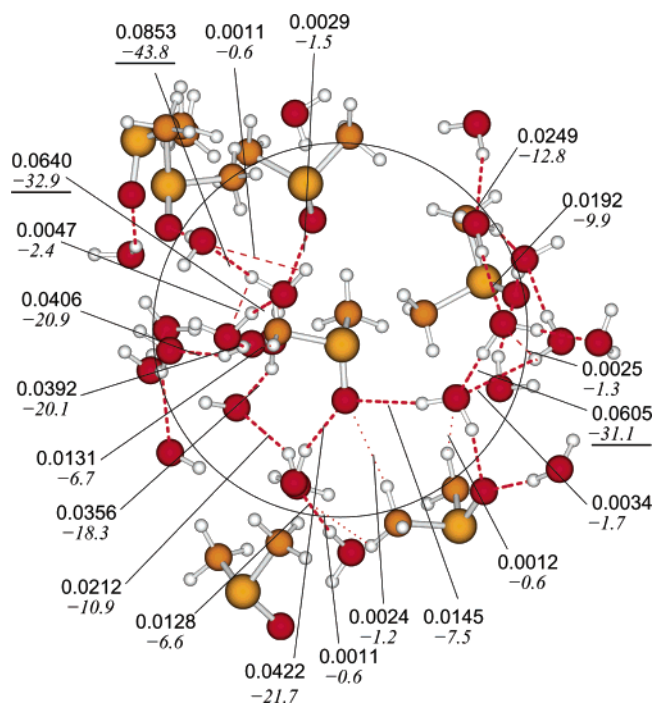


Figure 4. Snapshot from a DMSO–water CPMD simulation (152 atoms) with periodic boundary conditions taken from re 33 (the snapshot has been analyzed by a single-point B3LYP/TZVP calculation with TURBOMOLE). For all hydrogen bonds inside the black circle the SEN values and the corresponding attraction energies (in kJ/mol, italics) are given.

analyzed by heavily relying on geometric criteria (compare ref 34 for a recent example). Here, this standard approach is of great value as much experience has been gained with the empirical geometric criteria.

However, hydrogen bonding in proteins has been discussed very recently by Tjandra and collaborators³⁵ (see also references cited therein concerning geometric approaches to hydrogen bonding in proteins) who state that “It is assumed from small molecule studies that ideal hydrogen bonds have a linear orientation between donor proton and acceptor oxygen. However, the manner in which the hydrogen bond angle compensates for deviations from linearity has not been clearly detailed.” and “... an inquiry into the relationship between hydrogen-bond length and hydrogen-bond angle would provide a better understanding of hydrogen-bond geometry in proteins.” The SEN approach is able to provide detailed insight into this problem. As an example we choose an α -helix of 10 alanine amino acids (Figure 5), which comprises six intramolecular hydrogen bonds in its “idealized”-helical structure **2a** and seven in its relaxed structure **2b**.

Table 2 lists the geometric data for the six hydrogen bridges of **2a** and gives the corresponding SEN and $E_{H(amide)-O(carbonyl)}^{SEN}$ values. These data are compared with the B3LYP/TZVP results for the **2b** structure. First, it nicely demonstrates that SEN consistently predicts all hydrogen bonds in the “idealized”-helical structure **2a** to be of equal strength. In a MD simulation SEN can track the energetical change in these bridges and provides energetical data for structural changes in the peptide. Such changes are modeled by the relaxed structure **2b**, for which we note that the distances of the hydrogen-bonding contacts and also some of the connectivities have been changed upon relaxation. The original hydrogen bond with bond length r_6 was broken and a new one, r_6^* , has emerged. It is clear that these changes are already visible in the structural data, which show largely increased distances (by more than 300 pm) for the broken hydrogen bonds. The SEN approach immediately yields energetical values for the new and for the elongated hydrogen bridges.

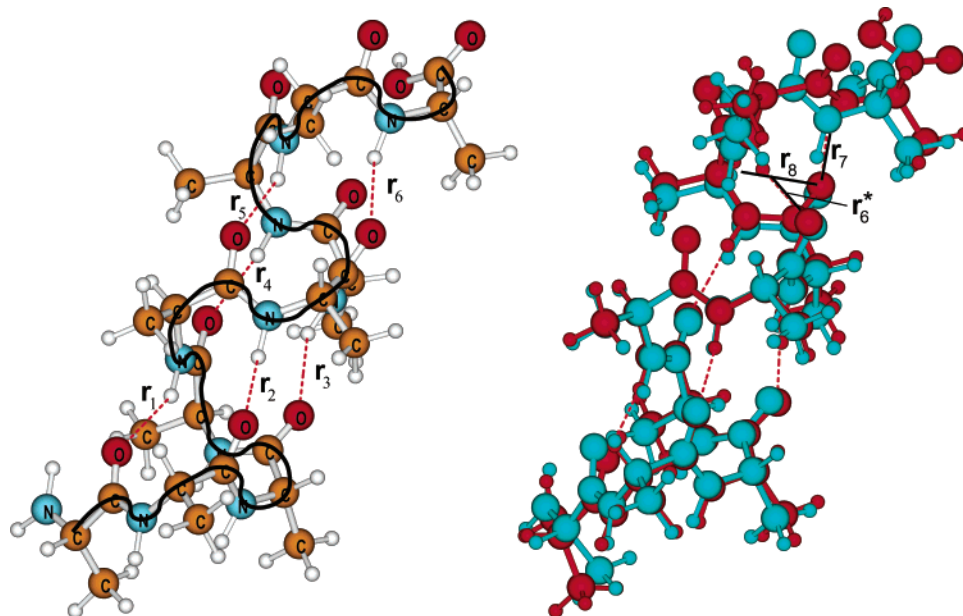


Figure 5. Left: Stabilization of a helical structure through 6 equidistant hydrogen bonds in an α -helix strand of 10 alanine amino acids **2a**. Right: Superposition of **2a** with a second, relaxed structure **2b** of the same helix.

TABLE 2: Structural Data (Hydrogen Atom Acceptor Distances $d(\text{HA})$ in pm and Corresponding Angles $a(\text{NHO})$ in Degrees) and SEN Interaction Energies $E_{\text{H}(\text{amide})-\text{O}(\text{carbonyl})}^{\text{SEN}}$ (in kJ/mol) for the Hydrogen Bridges in α -helices **2a and **2b** (B3LYP/TZVP)**

	$r(\text{HA})$	$a(\text{NHO})$	σ_{HA}	$E_{\text{H}(\text{amide})-\text{O}(\text{carbonyl})}^{\text{SEN}}$
2a:				
r ₁	210.4	151.6	0.0246	−12.6
r ₂	210.3	151.6	0.0231	−11.9
r ₃	210.4	151.6	0.0232	−11.9
r ₄	210.3	151.6	0.0234	−12.0
r ₅	210.4	151.6	0.0227	−11.7
r ₆	210.4	151.7	0.0224	−11.5
2b:				
r ₁	217.6	161.8	0.0154	−7.9
r ₂	209.7	162.0	0.0195	−10.0
r ₃	219.8	160.5	0.0183	−9.4
r ₄	226.9	149.6	0.0187	−9.6
r ₅	300.6	116.9	—	—
r ₆	339.3	98.8	—	—
r ₆ [*]	213.0	156.8	0.0192	−9.7
r ₇	216.7	157.3	0.0155	−8.0
	$r(\text{HA})$	$a(\text{CHO})$	σ_{HA}	$E_{\text{H}(\text{CH})-\text{O}(\text{carbonyl})}^{\text{SEN}}$
r ₈	262.6	89.1	0.0060	−3.1

The most important difference between **2b** and **2a** is the weak hydrogen bond with bond length r_8 , which was not visible in **2a**. This hydrogen bond involves the hydrogen atom directly attached to a carbon atom of the peptide's backbone. The SEN approach thus gives a direct indication that such weak hydrogen bonding interactions can play a role for classical protein dynamics, which, in general, focuses on hydrogen bonding interactions between $=\text{CO}$ and $=\text{NH}$ groups with predefined potentials. The importance of hydrogen bonds of this type within a peptide has recently been studied experimentally by Baures et al.³⁶ These authors emphasize with respect to a detection of such hydrogen bonds by geometric criteria that "It has been pointed out, however, that these geometric criteria are far too restrictive and should no longer be applied. Indeed, there are examples of $\text{C}-\text{H}\cdots\text{O}$ contacts that either do not fit these geometric criteria or do not show the spectroscopic changes expected for hydrogen bonded atoms." (See also the references for geometric criteria cited therein.) The wave function-based

criterion can thus serve as a valuable descriptor for such interactions in polypeptides.

5. Conclusion

The purpose of this work was to demonstrate that the increasing availability of wave functions for large many-atom systems in molecular dynamics simulations — either in CPMD simulations or in single-point calculations on MD snapshots — offers the ability to extract additional information on the system from its electronic structure. This additional information is intended to supplement the techniques which are currently available for analyses of MD data. The value of such additional tools becomes clear if systems are studied for which the standard MD tools have not been well developed.

The advantages of a wave-function-based criterion over a geometric criterion are similar to the advantages of Car–Parrinello simulations over traditional (i.e., based on predefined pair potentials) MD. Although in CPMD an unforeseen event can occur, traditional MD can show only what is a priori defined, in the sense that it has to be already present in the predefined pair potentials. The situation is similar for geometric criteria: it must be known in advance between which pair of functional groups or atoms an attractive interaction can be established and which geometrical arrangement is called attractive and which is not. For the correct detection of interactions in terms of geometric criteria, one would need to know the full potential energy surface of the pair of interacting molecules. Even if this surface is known, environmental effects are still missing. The interaction of molecules changes if they are solvated and if many-body effects play a role. Obviously, these aspects cannot all be mapped onto the set of rules representing the geometric criteria for the detection of attractive interactions, but a wave-function-based criterion is able to account for all of them.

We have discussed the semiquantitative SEN approach as an example for a wave-function-based criterion for the analysis of intermolecular interactions. It has been shown how the SEN approach can be utilized to gain useful insight into the intra- and intermolecular interaction dynamics of large complex systems. Two examples have been successfully studied by the SEN approach and were discussed in detail: (i) the different

types of hydrogen bonding in DMSO–water mixtures, in which methyl–hydrogen–water–oxygen contacts are to be detected, and (ii) the occurrence of C–H···O hydrogen bonds in polypeptides, which can hardly be detected by existing geometric criteria.

SEN can thus serve to support and supplement conclusions for interactions based on geometric criteria. To make the SEN approach more feasible for MD simulations, research is currently in progress to validate general (i.e., system-independent) distance-dependent approaches, which can correct for the unexact behavior of SEN in the attractive, nonequilibrium region of an interaction potential and for the inappropriate behavior at the repulsive side of the interaction potential.

Acknowledgment. We thank the German science foundation DFG and the Fonds der Chemischen Industrie for financial support.

References and Notes

- (1) Silverstein, K. A. T.; Haymet, A. D. J.; Dill, K. A. *J. Am. Chem. Soc.* **2000**, *122*, 8037–8041.
- (2) Southall, N. T.; Dill, K. A.; Haymet, A. D. J. *J. Phys. Chem. B* **2002**, *106*, 521–533.
- (3) Desiraju, G.; Steiner, T. The Weak Hydrogen Bond. In *Structural Chemistry and Biology*; International Union of Crystallography Monographs on Crystallography; Oxford University Press: Oxford, 1999; Vol. 9.
- (4) Grubbs, R. H.; Coates, G. W. *Acc. Chem. Res.* **1996**, *29*, 85–93.
- (5) Luzar, A.; Chandler, D. *Phys. Rev. Lett.* **1996**, *76*, 928–931.
- (6) Carloni, P.; Rothlisberger, U. Simulations of Enzymatic Systems: Perspectives from Car-Parrinello Molecular Dynamics Simulations. In *Theoretical Biochemistry: Processes and Properties of Biological Systems*; Elsevier: London, 2001; p 215.
- (7) Tarek, M.; Tobias, D. J. *Phys. Rev. Lett.* **2002**, *88*, 138101/1–4.
- (8) Chandler, D. *Nature* **2002**, *417*, 491.
- (9) Car, R.; Parrinello, M. *Phys. Rev. Lett.* **1985**, *55*, 2471–2474.
- (10) Reiher, M.; Sellmann, D.; Hess, B. A. *Theor. Chem. Acc.* **2001**, *106*, 379–392.
- (11) Ehrhardt, C.; Ahlrichs, R. *Theor. Chim. Acta* **1985**, *68*, 231–245.
- (12) Davidson, E. R. *J. Chem. Phys.* **1967**, *46*, 3320–3324.
- (13) Roby, K. R. *Mol. Phys.* **1974**, *27*, 81–104.
- (14) Heinzmann, R.; Ahlrichs, R. *Theor. Chim. Acta* **1976**, *42*, 33–45.
- (15) Ahlrichs, R.; Bär, M.; Häser, M.; Horn, H.; Kölmel, C. *Chem. Phys. Lett.* **1989**, *162*, 165–169.
- (16) Becke, A. D. *J. Chem. Phys.* **1993**, *98*, 5648–5652.
- (17) Stephens, P. J.; Devlin, F. J.; Chabalowski, C. F.; Frisch, M. J. *J. Phys. Chem.* **1994**, *98*, 11623–11627.
- (18) Schäfer, A.; Huber, C.; Ahlrichs, R. *J. Chem. Phys.* **1994**, *100*, 5829–5835.
- (19) Boys, S. F.; Bernardi, F. *Mol. Phys.* **1970**, *19*, 553–566.
- (20) van Duijneveldt, F. B.; van Duijneveldt-van de Rijdt, J. G. C. M.; van Lenthe, J. H. *Chem. Rev.* **1994**, *94*, 1873–1885.
- (21) Hutter, J.; et al. *CPMD*. IBM Research Division, Zürich Research Lab. and MPI für Festkörperforschung, Stuttgart, Stuttgart/Zürich, 1990–2001.
- (22) Hutter, J. private communication.
- (23) Eichkorn, K.; Treutler, O.; Öhm, H.; Häser, M.; Ahlrichs, R. *Chem. Phys. Lett.* **1995**, *240*, 283–290.
- (24) Eichkorn, K.; Weigend, F.; Treutler, O.; Ahlrichs, R. *Theor. Chem. Acc.* **1997**, *97*, 119–124.
- (25) Ochsenfeld, C.; White, C. A.; Head-Gordon, M. *J. Chem. Phys.* **1998**, *109*, 1663–1669.
- (26) Scuseria, G. E. *J. Phys. Chem. A* **1999**, *103*, 4782–4790.
- (27) Schütz, M.; Hetzer, G.; Werner, H.-J. *J. Chem. Phys.* **1999**, *111*, 5691–5705.
- (28) Kudin, K. N.; Scuseria, G. E. *Phys. Rev. B* **2000**, *61*, 16440–16453.
- (29) Kollmar, C.; Hess, B. A. *Mol. Phys.* **2002**, *12*, 1945–1955.
- (30) Weigend, F. *Phys. Chem. Chem. Phys.* **2002**, *4*, 4285–4291.
- (31) Berghold, G.; Parrinello, M.; Hutter, J. *J. Chem. Phys.* **2002**, *116*, 1800–1810.
- (32) Kirchner, B.; Reiher, M. *J. Am. Chem. Soc.* **2002**, *124*, 6206–6215.
- (33) Kirchner, B.; Hutter, J. *Chem. Phys. Lett.* **2002**, *364*, 497–502.
- (34) Margulis, C. J.; Stern, H. A.; Berne, B. J. *J. Phys. Chem. B* **2002**, *106*, 10748–10752.
- (35) Lipsitz, R. S.; Sharma, Y.; Brooks, B. R.; Tjandra, N. *J. Am. Chem. Soc.* **2002**, *124*, 10621–10626.
- (36) Baures, P. W.; Beatty, A. M.; Dhanasekaran, M.; Helfrich, B. A.; Pérez-Segarra, W.; Desper, J. *J. Am. Chem. Soc.* **2002**, *124*, 11315–11323.